JOURNAL OF THERMOPHYSICS AND HEAT TRANSFER
Vol. 23, No. 1, January–March 2009

Technical Notes

TECHNICAL NOTES are short manuscripts describing new developments or important results of a preliminary nature. These Notes should not exceed 2500 words (where a figure or table counts as 200 words). Following informal review by the Editors, they may be published within a few months of the date of receipt. Style requirements are the same as for regular contributions (see inside back cover).

Multidimensional Assessment of Modeling Error in Typical High-Speed Wind-Tunnel Heat-Transfer Data-Reduction Schemes

Benjamin S. Kirk*
NASA Lyndon B. Johnson Space Center, Houston, Texas 77058

DOI: 10.2514/1.35989

I. Introduction

RIGOROUS validation of computational tools places stringent demands on the accuracy of measured experimental data. This is increasingly the case in fluid dynamics, in which computational approaches have matured to the point at which certain properties may be predicted to the same level of accuracy that can be measured. In such a situation, a discrepancy between computation and experiment cannot simply be assumed to lie exclusively in either the computational or experimental result. Rather, a thorough evaluation of both the computational and experimental techniques is required. Such is the case for perfect-gas wind-tunnel measurements of surface heat transfer for a simple body in an attached laminar flow.

A standard technique for measuring the heat-transfer rate to a surface is via thermocouple instrumentation. The thermocouples may be subjected to an unknown heat flux for some period of time, and temperature histories may be obtained. This surface temperature history can then be used as a boundary condition in a transient thermal analysis from which the heat-transfer rate may be inferred. This technique is often employed in wind-tunnel tests that seek to quantify the aerothermodynamic environment for a given geometry. In such applications, the thermocouple instrumentation is typically too sparse to determine a true multidimensional surface temperature distribution, which could then be used in a three-dimensional thermal analysis. Consequently, the thermocouple temperature histories are often used in conjunction with a one-dimensional heat-transfer analysis, which only considers conduction normal to the surface. For geometries with regions of tight curvature and/or substantial lateral gradients in heat-flux distribution, the validity of the one-dimensional assumption comes into question.

This Note investigates the modeling error induced by the combined factors of lateral heat-flux distribution and multidimensional curvature for a specific geometry that was recently tested in the Arnold Engineering Development Center's Hypervelocity Wind Tunnel no. 9. A purely analytical approach is used that combines steady computational fluid dynamics simulation, transient three-dimensional thermal analysis, and the standard transient one-dimensional thermal analysis technique to quantify the modeling error introduced through the data-reduction process for each gauge. The remainder of the Note is organized as follows: Section II provides an overview of the experimental test series that provides the motivation for this work, Sec. III describes the analytical approach used to predict the external convective heat-transfer and the transient thermal analysis, Sec. IV presents results for the specific case of a scaled Orion Crew Module model at wind-tunnel conditions, and some general conclusions are discussed in Sec. V.

Received 2 December 2007; revision received 10 April 2008; accepted for publication 22 April 2008.

*Aerospace Engineer, Applied Aeroscience and Computational Fluid Dynamics Branch, 2101 NASA Parkway, Mail Code EG3.

II. Experimental Configuration

A recent test series was conducted in the Arnold Engineering Development Center's Hypervelocity Wind Tunnel no. 9 (HVWT9) with the primary intent of measuring laminar and turbulent convective heat-transfer rates on a scaled model of NASA's Orion Crew Module [1]. It is worthwhile to understand the experimental configuration as it provides the motivation for the subsequent analysis. HVWT9 is a conventional blowdown hypersonic wind tunnel with contoured nozzles capable of operation at nominal Mach numbers of 8, 10, and 14. A unique capability of the facility is the ability to run at very high Reynolds numbers (on the order of 131×10^6 1/m, or 40×10^6 1/ft). A typical run duration in HVWT9 is on the order of 1 s, which is sufficiently long such that thermal conduction into the model may become a concern [2].

The stainless steel model was instrumented with surface-mounted type-E Chromel thermocouples. The model and surface instrumentation is shown in Fig. 1 as installed in the tunnel. The temperature for each gauge was recorded during the course of a run. A one-dimensional explicit finite difference thermal analysis was performed for each gauge using the measured temperature as a surface boundary condition, and the heat transfer was inferred from the resulting temperature distribution. As mentioned previously, this is a standard data-reduction technique that is appropriate when a locally quasi-1-D assumption is valid.

The model diameter was chosen as 0.1778 m (7 in.) to allow for testing at a range of angles of attack without introducing tunnel blockage. Figure 2a shows a schlieren image of the model at an angle of attack during the course of a run at a freestream Mach number of 10. The model bow shock is clearly evident, as is a secondary shock produced by the model support sting.

Experimental data are compared with computational predictions in Fig. 2b, which is reproduced from Hollis et al. [1]. A cross section of the heat shield is shown with a black line in Fig. 2b for reference. The agreement between computation and experiment is quite good. The data for run 38 appear to be transitioning away from the laminar prediction for $z/R \geq 0$, which is to be expected for this higher Reynolds number. Still, for the shoulder gauges at $z/R = \pm 1$, there is some disagreement between the measurements and predictions. These data were reduced using the 1-D approach mentioned previously, and so the approach outlined in this Note may yield insight into this mismatch.

At high angles of attack there is a substantial spatial variation in the heat-transfer distribution around the windward shoulder of the vehicle. This heat-flux distribution and the relatively small radius of curvature of the shoulder both call into question the validity of the one-dimensional assumption used in the standard data-reduction technique. It should be pointed out that measurement of the peak heat

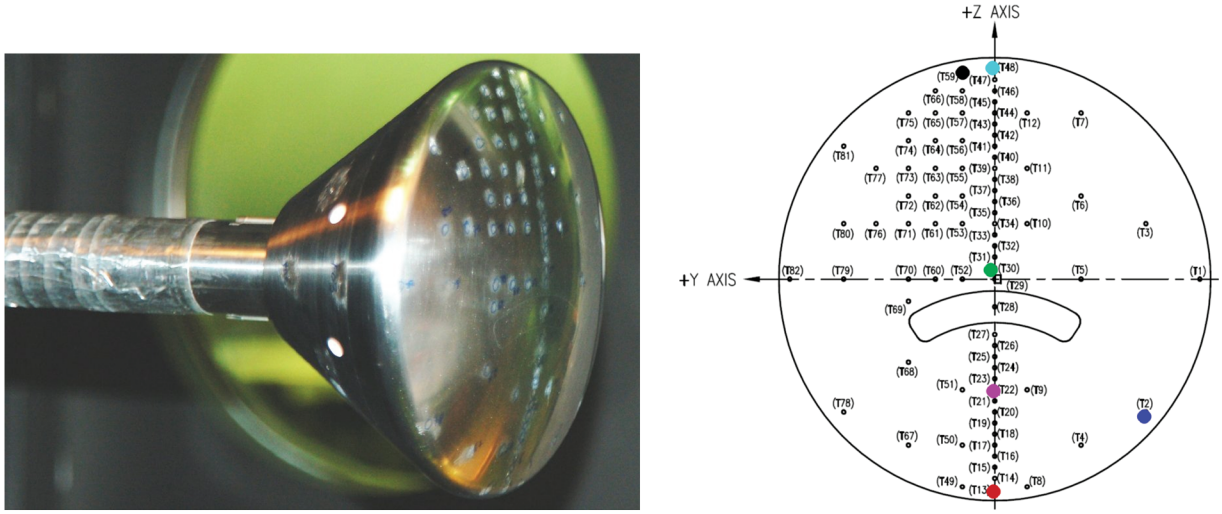

a) Orion crew module installed in the AEDC hypervelocity wind tunnel no. 9 test section **b) Instrumentation layout**

Fig. 1 Orion Crew Module 0.0357% model (AEDC is the Arnold Engineering Development Center).

flux on the shoulder region was not a primary goal of the test, and hence the instrumentation layout was not optimized for this region. Still, measurements were made in close proximity to the predicted peak heat-transfer location. These measurements are valuable for validating convective heat-transfer predictive capability, provided that the measurement error can be accurately quantified.

III. Methodology

A purely analytical approach was used in this analysis to assess the modeling error introduced through the 1-D data-reduction approach. In this technique, a known three-dimensional heat-flux distribution is obtained from a flowfield solution. This heat flux is then applied as a mixed boundary condition in a transient 3-D thermal analysis. The surface temperature history is then extracted and provides a surrogate data set for use with the 1-D reduction methodology. The (known) input heat flux is then compared with the output heat flux from the 1-D reduction methodology to directly assess the modeling error inherit in the experimental data-reduction technique.

Specifically, the approach used was as follows:

1) A representative heat-transfer coefficient distribution was obtained from a computational fluid dynamics analysis.

2) This heat-transfer coefficient was used as a boundary condition in a transient thermal analysis spanning the length of a typical wind-tunnel run.

3) The surface temperature history was extracted from the thermal analysis for each gauge location.

4) These temperature histories were used in a 1-D data-reduction analysis as data.

5) A comparison of the predicted-vs-known heat-flux histories provided a measure of the modeling error.

Another possibility for the three-dimensional analysis would be to solve the problem coupled in time. In this approach, the fluid dynamic and thermal simulations would proceed in parallel with coupling at each time step. Although physically more correct, this approach was deemed unnecessary for the goals of assessing modeling error. This is because it has been previously shown that an assumed (fixed) wall temperature has little influence on the heat-transfer coefficient distribution for the wall-temperature ranges expected in a typical wind-tunnel run [3].

A. External Convective Heat Transfer

Computational fluid dynamics (CFD) analysis was performed for the specific case of Mach 9.82 with a diameter-based Reynolds

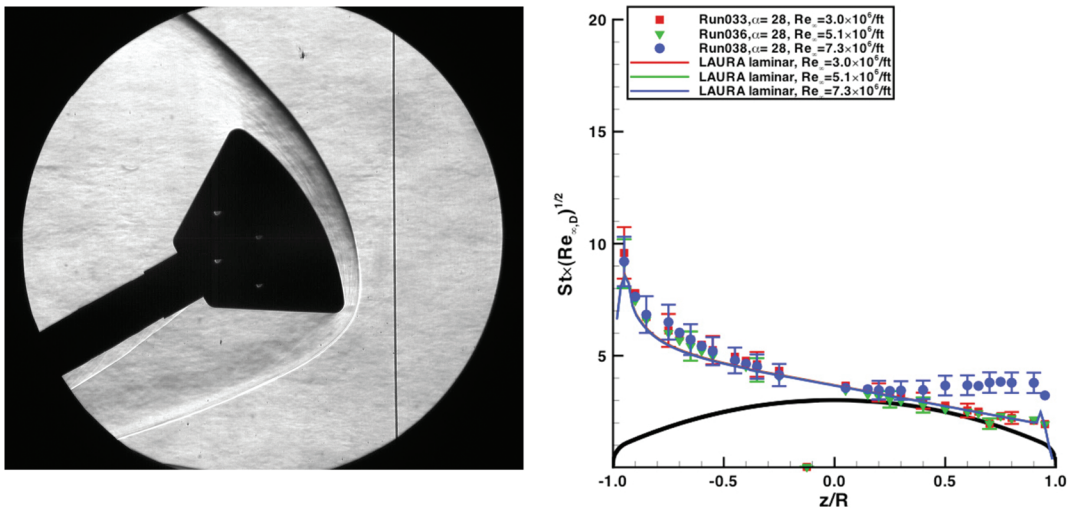

a) Experimental schlieren image **b) Measured and predicted heat-transfer distributions [1]**

Fig. 2 Experimental results.

number $Re_D = 2.33 \times 10^6$ perfect-nitrogen flow over an isothermal model at a 28 deg angle of attack. The surface temperature was assumed to be fixed at 26.8°C (80°F). Sutherland's law was used to obtain the fluid viscosity. The fluid's thermal conductivity was then obtained by the assumption of a constant Prandtl number. The simulation was performed with the Data Parallel Line Relaxation code [4], which uses a block-structured finite volume methodology to discretize the thermochemical nonequilibrium Navier–Stokes equations and is widely used in the aerothermodynamics community [5–7].

The resulting heat-transfer distribution is shown in Fig. 3. A cross section of the heat shield is shown with a black line in Fig. 3b for reference. It is clear from the centerline distribution that the heat-transfer distribution exhibits considerable local variation, particularly in the shoulder regions of maximum curvature ($z/R = \pm 1$). Note that the high spatial variation in the heat flux and surface curvature in these regions render the one-dimensional data-reduction approach suspect.

B. Thermal Analysis

1. Mathematical Model

The transient temperature distribution $T(t)$ in a conducting medium is given by [8]

$$\rho c_p \frac{\partial T}{\partial t} = \nabla \cdot (k \nabla T) \tag{1}$$

where ρ, c_p, and k are the material density, specific heat, and thermal conductivity, respectively, and t denotes time. In this work, we restrict our attention to the case of an isotropic medium in which the specific heat and conductivity are both functions of temperature.

Equation (1) is solved numerically on two distinct domains for this analysis. A calculation is first performed for the entire heat shield. This multidimensional analysis accounts for the combined effects of model curvature and nonuniform external heat-transfer distribution. The second domain is a one-dimensional segment for which the length corresponds to the model wall thickness. This 1-D analysis ignores any model curvature or heat-flux distribution effects, which is consistent with the approach used in typical wind-tunnel data-reduction analysis.

2. Material Properties

The density, thermal conductivity, and specific heat used to model 17-4PH stainless steel are

$$\rho = 0.282 \text{ lbm/in.}^3 = 7.806 \text{ g/cm}^3 \tag{2}$$

$$k = 2.08 \times 10^{-4} + 1.06 \times 10^{-7} \text{ T Btu/in.s°F} \approx 0.156 \text{ W/cm°C} \tag{3}$$

$$c_p = 0.104 + 3.38 \times 10^{-5} \text{ T} + 4.45 \times 10^{-8} \text{ T}^2 \text{ Btu/lbm°F} \approx 0.435 \text{ J/g°C} \tag{4}$$

The thermal conductivity and specific heat are both weak functions of temperature for the range of temperatures experienced during a typical wind-tunnel run, yielding Eq. (1) nonlinear.

3. Numerical Method

A symmetric Galerkin weak form for Eq. (1) follows from multiplying by a suitable test function v, integrating over the domain Ω, and applying the Gauss divergence theorem [9]. The weak form is then as follows: Find $T \in H^1$, satisfying the given initial and boundary conditions such that

$$\int_\Omega \left(\rho c_p \frac{\partial T}{\partial t} v + k \nabla T \cdot \nabla v \right) d\Omega - \oint_{\partial \Omega_N} (k \nabla T \cdot \hat{n}) v d\Gamma = 0 \tag{5}$$

for all $v \in H_0^1$. The boundary integral term may be replaced with Fourier's law:

$$\dot{q} = -k \nabla T \tag{6}$$

which allows Eq. (5) to be rewritten in terms of the wall heat flux $\dot{q}_w = \dot{q} \cdot \hat{n}$:

$$\int_\Omega \left(\rho c_p \frac{\partial T}{\partial t} v + k \nabla T \cdot \nabla v \right) d\Omega + \oint_{\partial \Omega_N} \dot{q}_w v d\Gamma = 0 \tag{7}$$

This weak form is then discretized with a standard finite element approach and implemented in the parallel adaptive `libMesh` [10] library. Piecewise linear finite elements are used for the spatial discretization, and the temporal discretization is performed with a centered Crank–Nicolson scheme [11]. The resulting scheme is second-order-accurate in both space and time. The very weak nonlinearity introduced by the material properties is treated with a standard Newton scheme. The heat-shield portion of the wind-tunnel model was discretized using a hybrid-element unstructured mesh, as shown in Fig. 4.

4. Boundary Conditions

In the 3-D analysis, the exposed surface of the heat shield is subjected to a convective heat flux for which the magnitude is taken from the CFD analysis. The remainder of the surfaces are treated as adiabatic. The CFD analysis was performed for an isothermal wall

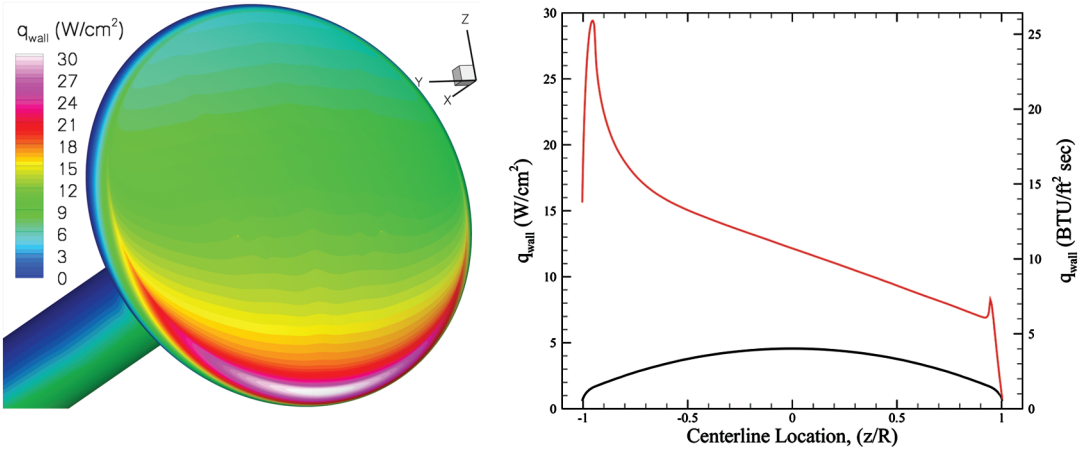

a) Heat-shield distribution **b) Centerline distribution**

Fig. 3 Surface heat-transfer distribution obtained from CFD analysis.

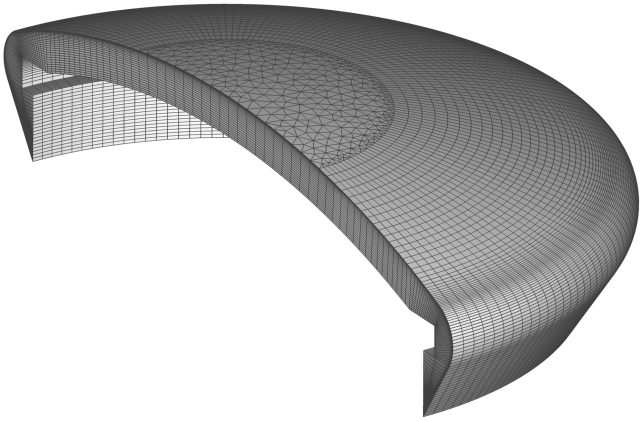

Fig. 4 Heat-shield finite element model.

condition. The resulting heat-flux distribution and fixed wall temperature were used to derive a heat-transfer coefficient h:

$$h = \frac{\dot{q}_w}{T_0 - T_w} \tag{8}$$

where T_0 is the freestream total temperature, T_w is the wall temperature assumed in the CFD analysis, and $\dot{q}_w$ is the heat transfer computed from the CFD simulation. The heat-transfer coefficient varies spatially over the exposed surface of the model, but this spatial distribution is assumed to be constant during the course of a run. The transient heat transfer is then applied in the thermal analysis and is a function of surface temperature:

$$\dot{q}(t) = h(T_0 - T(t)) \tag{9}$$

This mixed boundary condition is used in the boundary integral in Eq. (7) to weakly impose the specified heat flux on the wetted surface of the model. The adiabatic condition is also enforced weakly on the remaining surfaces by simply omitting the boundary integral term in the computation.

In the 1-D analysis, temperature histories were obtained from the 3-D thermal analysis for each gauge location. These histories were then used as Dirichlet boundary conditions in 1-D thermal analysis for consistency with the approach used in the experimental data reduction. In this way, the 3-D thermal analysis provides a synthetic data set that can be used to perform the standard 1-D data-reduction process. Further, because the applied heat flux is known for the 3-D analysis, it may be compared with the heat flux obtained from the 1-D analysis for an assessment of data-reduction modeling error for each gauge.

C. Modeling Error

With the surface temperature specified as a function of time, the transient 1-D analysis may be performed. The transient heat flux measured at the surface can then be determined and compared with the (known) applied heat flux from the 3-D simulation. This allows the modeling error imposed by the 1-D assumption to be directly computed as

$$e = \frac{\dot{q}_{\text{measured}} - \dot{q}_{\text{applied}}}{\dot{q}_{\text{applied}}} \tag{10}$$

for each gauge.

IV. Results

A. Thermal Analysis

The heat-transfer distribution shown previously in Fig. 3 was used to define a heat-transfer coefficient as described in Sec. III. The model was then simulated for a duration of 1 s from a uniform initial temperature of 26.8°C (80°F), which is consistent with the length of a typical run in HVWT9. Results for this simulation are shown in Fig. 5.

The temperature distribution is shown on both the surface of the model and in the plane of symmetry in Fig. 5a. As expected, the surface temperature distribution is visually similar to the applied heat-flux distribution, albeit somewhat smoothed through thermal diffusion.

Further, the depth to which the temperature profile has penetrated the model surface agrees qualitatively with dimensional analysis. The thermal diffusivity α is defined as

$$\alpha = \frac{k}{\rho c_p} \tag{11}$$

and has units of in.^{2}/s. From inspection of Eq. (1), it is clear that

$$\frac{\Delta T}{\Delta t} \propto \alpha \frac{\Delta T}{\Delta x^2} \tag{12}$$

or, equivalently,

$$\Delta x \propto \sqrt{\alpha \Delta t} \tag{13}$$

This simple dimensional analysis predicts that the thermal layer will have penetrated approximately 16% into the model wall, which is in qualitative agreement with Fig. 5a.

The surface temperature history is shown for several thermocouple locations in Fig. 5b. (Note that the gauge locations are depicted schematically with the symbols in Fig. 1b.) The surface temperature was extracted in a similar way for all gauge locations on the heat shield for use in assessing the modeling error in the 1-D data-reduction scheme. The surface response for the peak heat-flux gauge location displays the classic $\sqrt{t}$ behavior that is characteristic of

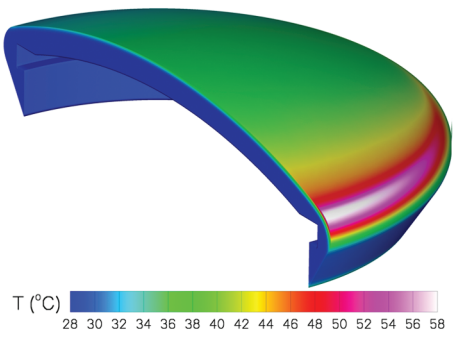

a) Temperature distribution throughout the heat shield after 0.5 s

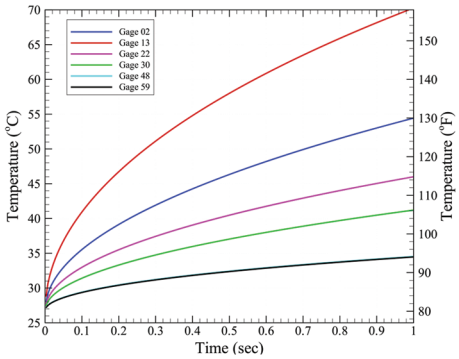

b) Temperature history for the peak heat-flux gauge

Fig. 5 Heat-shield temperature distribution and gauge history.

conduction in an infinite slab with constant surface heat flux [12]. This qualitative behavior suggests that using a 1-D data-reduction scheme would be fairly accurate, as will be shown in the following section.

B. Modeling Error

The modeling-error history was computed for six select gauge locations. The gauge locations are illustrated in Fig. 1b. Two of the gauges are located on the windward shoulder of the heat shield, two are on the leeward shoulder, and the remaining two are on the heat-shield acreage. By inspection of the geometry and the applied heat-flux distribution, it is expected that the two acreage gauges would have the lowest modeling error.

The modeling-error history for these gauges is shown in Fig. 6. As expected, the minimum error occurs for the two acreage gauges, which is approximately $\pm\frac{1}{2}\%$. This is consistent with the relatively uniform applied heat flux and low radius of curvature in this region.

The modeling error for the two windward gauges is substantially larger at approximately 2 to 5%. The magnitude of the error increases with time, presumably due to lateral conduction induced by the applied heat-flux distribution. The modeling error for the two leeward gauges is approximately -2 to -6% during the simulated period of interest. It is somewhat surprising that the error for the windward shoulder gauges (2 and 13) is actually less than the leeward shoulder gauges (48 and 59) at later times, especially given that the variation in applied heat flux is clearly larger at the windward shoulder (cf. Fig. 3b). However, some insight may be gained from the observation that the leeward gauges tend to read low, in that the 1-D data-reduction approach yields a lower heat flux than was actually applied. This behavior may be attributed to important lateral conduction effects. Because the majority of the heat shield is hotter than this leeward shoulder, there will be conduction toward these gauges within the heat shield. Consequently, the steel in the vicinity of the leeward shoulder will be hotter than it would be in the absence of this lateral conduction effect. The end result may be that this warmer substrate is more resistive to heat flow than in the absence of the multidimensional conduction, therefore requiring more heat flux at the surface to affect the same response. In this way, the leeward shoulder gauges read low. These results are qualitatively consistent with the data shown in Fig. 2b, which were reduced using the 1-D approach. This analysis would suggest that the windward shoulder gauge data are high, whereas the leeward shoulder data are low. This is in qualitative agreement with the predicted values at these locations.

It is interesting to note that this approach yields not only a gauge-by-gauge assessment of the modeling error introduced through the 1-D data-reduction assumption, but also provides insight into the bias that is introduced. This raises the possibility of using this approach to actually correct for the bias in the wind-tunnel data reduction. Specifically, it is clear from the figure that a standard 1-D data-reduction technique applied to the windward shoulder gauges will consistently overpredict the actual heat flux by approximately 2 to 5%. Conversely, the leeward shoulder gauges would be expected to underpredict the heat flux by 2 to 6%, depending on the duration of the wind-tunnel run.

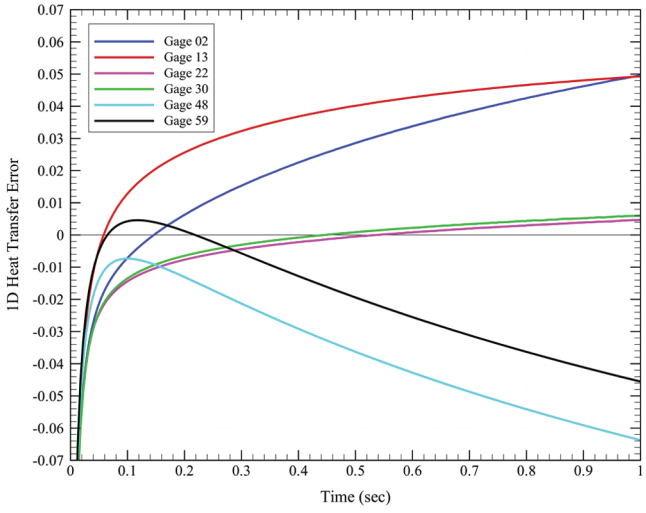

Fig. 6 Error history for select gauges.

It is important to note that the modeling error at these shoulder gauges is of the same order as the heat-transfer measurement error reported by wind-tunnel facilities. This suggests that an approach such as outlined here is worthwhile for obtaining the maximum utility from measured data for thermocouple-instrumented models with appreciable surface curvature. This is expected to be increasingly the case in the future as advances in both computational and experimental techniques continue to challenge each other to obtain high-accuracy validation data for increasingly complex configurations.

V. Conclusions

This Note presented a purely analytical approach for assessing the modeling error introduced by standard wind-tunnel data-reduction techniques for thermocouple-instrumented models. The specific example considered was a scaled model of NASA's Orion Crew Module at wind-tunnel conditions in the Arnold Engineering Development Center's Hypervelocity Wind Tunnel no. 9. This work was motivated primarily by the desire to obtain highly accurate heat-transfer data for validation of computational predictive capability.

A two-stage approach was outlined in which a multidimensional heat-transfer analysis is first performed for the specific model geometry using a heat-transfer coefficient boundary condition derived from a computational fluid dynamics simulation. This high-fidelity analysis then provides surface temperature data as a function of time. Next, these surface temperature histories are used as a synthetic data set in a standard one-dimensional data-reduction scheme. A comparison of the measured heat-transfer distribution and the known applied heat-transfer distribution then provides a measure of the data-reduction modeling error.

This work presented results for six distinct gauge locations on the Orion heat shield. Two of these gauges were located on the heat-shield acreage, for which the geometric radius of curvature is high and the spatial variation in applied heat flux is low. As expected, the modeling error for these gauges was very low ($\pm\frac{1}{2}\%$). The other four gauges were located on the shoulder of the heat shield, for which the radius of curvature is small and the variation in applied heat flux is high. For these gauges, the modeling error was on the same order of typical measurement errors ($\pm 5\%$).

This approach has the ability to identify the gauge-by-gauge bias introduced through the one-dimensional data-reduction approach for a specific geometry. This raises the possibility of using this approach to correct for this bias. For the specific case considered in this work, it was found that the standard data-reduction approach will overpredict the heat transfer on the windward shoulder of the vehicle while underpredicting the leeward shoulder values. It is believed that analyses such as presented in this Note will become increasingly important as computational tools require more stringent error quantification for validation data.

References

[1] Hollis, B. R., Berger, K. T., Horvath, T. J., Coblish, J. J., Norris, J. D., Lillard, R. P., and Kirk, B. S., "Aeroheating Testing and Predictions for Project Orion CEV at Turbulent Conditions," 46th AIAA Aerospace Sciences Meeting and Exhibit, AIAA Paper 2008-1226.

[2] Ragsdale, W. C., and Boyd, C. F., "Hypervelocity Wind Tunnel 9 Facility Handbook," 3rd ed., Naval Surface Warfare Center TR 91-616, Silver Spring, MD, July 1993.

[3] Kirk, B. S., "Adaptive Finite Element Simulation of Flow and Transport Applications on Parallel Computers," Ph.D. Thesis, Univ. of Texas at Austin, Austin, TX, May 2007.

[4] Wright, M. J., Candler, G. V., and Bose, D., "A Data-Parallel Line Relaxation Method for the Navier-Stokes Equations," *AIAA Journal*,

Vol. 36, No. 9, 1998, pp. 1603–1609.
doi:10.2514/2.586

[5] MacLean, M., and Holden, M., "Validation and Comparison of WIND and DPLR Results for Hypersonic, Laminar Problems," 42nd AIAA Aerospace Sciences Meeting and Exhibit, AIAA Paper 2004-529.

[6] Coblish, J. J., Smith, M. S., Hand, T., Candler, G. V., and Nompelis, I., "Double-Cone Experiment and Numerical Analysis at AEDC Hypervelocity Wind Tunnel No. 9," 43rd AIAA Aerospace Sciences Meeting and Exhibit, AIAA Paper 2005-0902.

[7] Nompelis, I., Candler, G. V., and Holden, M. S., "Effect of Vibrational Nonequilibrium on Hypersonic Double-Cone Experiments," *AIAA Journal*, Vol. 41, No. 11, November 2003, pp. 2162–2169.
doi:10.2514/2.6834

[8] Tannehill, J. C., Anderson, D. A., and Pletcher, R. H., *Computational Fluid Mechanics and Heat Transfer*, 2nd ed., Taylor & Francis, Washington, D.C., 1997.

[9] Becker, E. B., Carey, G. F., and Oden, J. T., *Finite Elements—An Introduction*, Vol. 1, Prentice–Hall, Upper Saddle River, NJ, 1981.

[10] Kirk, B. S., Peterson, J. W., Stogner, R. H., and Carey, G. F., "libMesh: A C++ Library for Parallel Adaptive Mesh Refinement/Coarsening Simulations," *Engineering with Computers*, Vol. 22, No. 3, 2006, pp. 237–254.
doi:10.1007/s00366-006-0049-3

[11] Crank, J., and Nicolson, P., "A Practical Method for Numerical Evaluation of Solutions of Partial Differential Equations of Heat Conduction Type," *Proceedings of the Cambridge Philosophical Society (Mathematical and Physical Sciences)*, Vol. 43, 1947, pp. 50–64.

[12] Sanderson, S. R., "Shock Wave Interaction in Hypervelocity Flow," Ph.D. Thesis, California Inst. of Technology, Pasadena, CA, May 1995.